Molecular Vision 2017; 23:103-115 <http://www.molvis.org/molvis/v23/103>
Received 17 October 2016 | Accepted 10 March 2017 | Published 12 March 2017

Differential responses of choroidal melanocytes and uveal melanoma cells to low oxygen conditions

Cindy Weidmann,[1,2] Jade Pomerleau,[1,2] Laurence Trudel-Vandal,[1,2] Solange Landreville[1,3]

[1]Axe Médecine régénératrice and Centre Universitaire d'Ophtalmologie (CUO)-Recherche, Centre de recherche du CHU de Québec, Quebec City, QC, Canada; [2]Centre de recherche en organogénèse expérimentale de l'Université Laval/LOEX, Quebec City, QC, Canada; [3]Département d'ophtalmologie, Faculté de médecine, Université Laval, Quebec City, QC, Canada

Purpose: Tissue culture is traditionally performed at atmospheric oxygen concentration (21%), which induces hyperoxic stress, as endogenous physiologic oxygen tension found in tissues varies between 2% and 9%. This discrepancy may lead to misinterpretation of results and may explain why effects observed in vitro cannot always be reproduced in vivo and vice versa. Only a few studies have been conducted in low physiologic oxygen conditions to understand the development and differentiation of cells from the eye.

Methods: The aim of this study was to investigate the growth and gene expression profile of melanocytes from the choroid permanently exposed to 21% (hyperoxic) or 3% (physiologic) oxygen with proliferation assays and DNA microarray. The cellular behavior of the melanocytes was then compared to that of cancer cells.

Results: The gross morphology and melanin content of choroidal melanocytes changed slightly when they were exposed to 3% O_2, and the doubling time was statistically significantly faster. There was an increase in the percentage of choroidal melanocytes in the active phases of the cell cycle as observed by using the proliferation marker Ki67. The caveolin-1 senescence marker was not increased in choroidal melanocytes or uveal melanoma cells grown in hyperoxia. In comparison, the morphology of the uveal melanoma cells was similar between the two oxygen levels, and the doubling time was slower at 3% O_2. Surprisingly, gene expression profiling of the choroidal melanocytes did not reveal a large list of transcripts considerably dysregulated between the two oxygen concentrations; only the lactate transporter monocarboxylate transporter (MCT4) was statistically significantly upregulated at 3% O_2.

Conclusions: This study showed that the oxygen concentration must be tightly controlled in experimental settings, because it influences the subsequent cellular behavior of human choroidal melanocytes.

Oxygen (O_2) plays a fundamental role in the metabolism of living cells. However, some O_2 derivatives, such as reactive oxygen species (ROS), can induce replicative senescence when produced in excess, presumably because of irreversible damage to nucleic acids, lipids, and proteins [1-3]. Oxygen concentrations greatly influence several physiologic and pathophysiological processes through the transcription factors hypoxia inducible factor 1 and 2 (HIF1A and HIF2A) that mediate the adaptive responses required for oxygen homeostasis [4-6]. Although oxygen is supplied to the tissues and cells at reported concentrations varying between 2% and 9% (about 15–70 mmHg) [7,8], current cell culture practices rely on incubators where the oxygen concentration corresponds to the atmospheric level (21% O_2 or 160 mmHg). Thus, the oxygen concentration used to expand cells in vitro effectively mimics hyperoxic conditions. Previous studies have shown that the viability and specialized functions of differentiated cells and stem cells are optimal at low physiologic oxygen concentrations that simulate the physiologic conditions of native tissues or stem cell niches [9-18].

The choroid of the eye is localized below the light-sensitive retina and contains melanocytes, which are melanin-pigmented cells derived from the neural crest [19,20]. Ocular melanin is believed to protect the eye against several ocular diseases by absorbing light, chelating metal ions, and quenching ROS [21,22]. The choroid is mainly exposed to visible light rather than ultraviolet (UV) but is highly vascularized and thus experiences significant oxidative stress [23]. The function of melanocytes in this tissue is not yet fully elucidated. These cells can be obtained from the choroid layer of donated eyes. In vitro culture of choroidal melanocytes has been routinely performed in incubators under atmospheric oxygen concentration [24,25], while in situ, these cells are not exposed to such a hyperoxic environment. Values below 12% O_2 were observed in the posterior segment of the eye as measured in the macaque retina and choroid [26-28]. Optimizing the in vitro expansion of choroidal melanocytes is essential to study their physiologic roles in the choroid and

Correspondence to: Solange Landreville, Hôpital du Saint-Sacrement, 1050 Chemin Sainte-Foy, Room H2-02, Centre de recherche du CHU de Québec, Quebec City, QC, G1S 4L8, Canada; Phone: (418) 682-7693; FAX: (418) 682-8000; email: Solange.Landreville@fmed.ulaval.ca

pathologies, such as uveal melanoma (UM) and age-related macular degeneration.

The purpose of this study was to investigate how an oxygen concentration that more closely reflects a physiologic condition (3% O_2) influences the molecular and cellular behaviors of human choroidal melanocytes. To achieve this, the morphology, cell proliferation, and gene expression profile were evaluated in choroidal melanocytes permanently grown at 21% or 3% O_2 and then compared to cancer cells. The analyses showed that low physiologic oxygen conditions improved the expansion of melanocytes from the choroid by shortening their doubling time and increasing their proliferative capacity, in contrast to UM cells, as well as by upregulating the expression of the lactate transporter monocarboxylate transporter (MCT4). We report for the first time transcriptome data from choroidal melanocytes expanded under a physiologic oxygen concentration.

METHODS

Human choroidal melanocyte cell culture: This study followed the tenets of the Declaration of Helsinki, adhered to the ARVO statement on human subjects, and was approved by our institutional human experimentation committee (Centre de recherche du CHU de Québec, Quebec City, Canada). Melanocytes were isolated from the choroid of three donor eyeballs (82, 51, and 83 years old; Centre universitaire d'ophtalmologie's (CUO) Eye Bank, Quebec City, Canada) by successive digestion in trypsin and collagenase [25]. Written informed consent for research purposes was obtained from the donor's next-of-kin. The isolated cells were then divided into equal parts and permanently exposed to two oxygen conditions: hyperoxia (21% O_2, 74% N_2, and 5% CO_2) in a CO_2 incubator (Sanyo; ESBE Scientific, St.-Laurent, Canada) and low physiologic oxygen conditions (3% O_2, 92% N_2, and 5% CO_2) in a multigas incubator (Sanyo; ESBE Scientific). Choroidal melanocytes (early passages, P2–P6) were grown for all experiments using FNC Coating Mix (AthenaES, Baltimore, MD), and Ham's F12 medium supplemented with 10% fetal bovine serum (FBS; Hyclone, Logan, UT), 10 ng/ml cholera toxin (Sigma-Aldrich, St. Louis, MO), 100 nM phorbol 12-myristate 13-acetate (Sigma-Aldrich), 100 µg/ml geneticin (Wisent, Quebec City, QC), and 50 µg/ml gentamicin [25,29]. The morphology and purity of the cultures were confirmed with microscopic inspection in phase contrast and Melan-A immunostaining (MLANA, also known as MART-1; mouse monoclonal, clone A103, prediluted; Dako, Mississauga, Canada). Human UM primary cultures (T111, T131, and T132) were derived from ocular tumor biopsies collected at the time of enucleation (Appendix 1; Clinique des tumeurs oculaires du CHU de Québec, Quebec City, Canada). Written informed consent was obtained from the enucleated subjects. UM cells (early passages, P8–P12) were grown for all experiments in Dulbecco's Modification of Eagle's Medium (DMEM) Low Glucose medium (Wisent) supplemented with 5% FBS (Hyclone) and 50 µg/ml gentamicin. MLANA immunostaining was performed on paraformaldehyde-fixed paraffin-embedded UM cell pellets following a technique of diaminobenzidine (DAB) biotin-streptavidin complex formation (Appendix 2) [30].

Cell count and doubling time: Choroidal melanocyte and UM cell numbers were compared between the 21% and 3% oxygen conditions using a cell and particle counter (Z2; Beckman Coulter, Mississauga, Canada). The cell counts were performed at each of three consecutive passages. The doubling time was determined using the initial number of cells, final number of cells, and duration of culture in hours (Roth V. 2006).

Anchorage-independent colony formation assay: Choroidal melanocytes (n = 3) and UM cells (n = 3) were plated in 1.3% methylcellulose (R&D Systems; Cedarlane, Burlington, Canada) on untreated 35 mm tissue culture dishes as previously described (melanocytes: 10,000 cells per triplicate; UM cells: 1,500–3,000 cells per triplicate) [31]. After 14 days of growth at 21% or 3% O_2, the colonies were stained with 0.1 mg/ml 3-(4,5-dimethylthiazol-2-yl)-2,5-diphenyltetrazolium bromide (MTT; Sigma-Aldrich) and counted with the Quantity One software version 4.3.0 (Bio-Rad Laboratories) using the Colony Counting tool.

Cell proliferation assay and cell nucleus characteristics: The choroidal melanocytes (n = 3) and UM cells (n = 3) grown at 21% or 3% O_2 were plated on coverslips (20,000 cells/coverslip), fixed 15 min with 4% paraformaldehyde after 24 h of plating, and permeabilized with 0.1% Triton X-100. The blocking of nonspecific sites was performed with 5% goat serum in PBS (1X; 137 mM NaCl, 2.7 mM KCl, 6.5 mM $NaHPO_4$, 1.5 mM KH_2PO_4, 0.9 mM $CaCl_2$, 0.5 mM $MgCl_2$, pH 7.4)/0.1% Triton X-100. To target choroidal melanocytes in the active phases of the cell cycle, immunostaining was performed with a primary antibody against the proliferation marker Ki67 (mouse monoclonal, clone MIB1, 1:400; BD PharMingen, Mississauga, Canada), followed by incubation with a secondary antibody anti-mouse-Alexa 488 for visualization (1:500; Life Technologies, Burlington, Canada). Mitotic UM cells were targeted with a primary antibody against the phosphorylated form of histone H3 (PH3; rabbit polyclonal, 1:1,600; Cell Signaling, Danvers, MA), followed by incubation with a secondary antibody anti-rabbit-Alexa 488 for visualization (1:500; Life Technologies). Nuclei were

counterstained with 4',6-diamidino-2-phenylindole (DAPI) nuclear stain (Life Technologies). Pictures of eight random fields on duplicate coverslips were taken on an epifluorescence microscope at 20X magnification (AxioImager 2; Zeiss, Toronto, Canada). The Ki67- or PH3-positive cells were counted, as well as the total number of nuclei for normalization. DAPI image post-processing was performed in ImageJ version 1.46r to determine the area (μm^2) and circularity of the nuclei ($4\pi \times [Area]/[Perimeter]^2$; the ranges were from 0 (infinitely elongated polygon) to 1 (perfect circle) [32]) in the choroidal melanocytes exposed to 21% or 3% O_2 (n = 3). A minimum of 500 nuclei was measured per condition with the Analyze Particules function.

Gene expression profiling: Total RNA was extracted from the choroidal melanocytes exposed to 21% or 3% O_2 (n = 3) by using the RNeasy Mini Kit (Qiagen, Toronto, Canada). The quantity and quality of total RNA were assessed using the 2100 Bioanalyzer and RNA 6000 Nano LabChip kit (Agilent Technologies, Mississauga, Canada). Gene expression profiling was performed by the Plateforme de génétique moléculaire du CUO-Recherche (Quebec City, Canada) using a SurePrint G3 Human GE 8×60K array slide (60,000 probes; Agilent Technologies). Cyanine 3-CTP labeled cRNA targets were prepared from 25 ng of total RNA using the Agilent One-Color Microarray-Based Gene Expression Analysis kit (Agilent Technologies). Then, 600 ng cRNA were incubated on the array slide. The slide was scanned on an Agilent SureScan Scanner according to the manufacturer's instructions (Agilent Technologies). Data were analyzed using the ArrayStar version 12 software (DNASTAR, Madison, WI) and were preprocessed using robust multiarray analysis and quantile normalization to obtain the expression measure for each probe set to generate scatterplots and heatmaps of selected mRNA of interest [29,33]. The color scale used in the heatmaps to display the $\log_2$ expression level values was determined by the Hierarchical clustering algorithm of the Euclidian metric distance between genes. The housekeeping mRNA golgin A1 (GOLGA1), C-terminal binding protein 1 (CTBP1), and beta-2-microglobulin (B2M) were used as internal controls to normalize the linear signals of the selected mRNA of interest [34]. Microarray data have been deposited in the NCBI's Gene Expression Omnibus (GEO) repository and are accessible through the Series record GSE86789.

Western blotting: Choroidal melanocytes and UM cells grown under hyperoxia or low physiologic oxygen conditions were harvested with radioimmunoprecipitation assay (RIPA) buffer supplemented with a protease inhibitor cocktail (Roche Diagnostics, Mississauga, Canada) for total protein extraction. The protein concentration was determined with the BCA protein assay kit (Pierce; Fisher Scientific) using dilutions of bovine serum albumin for the standards. Western blots were performed with 20 µg of total proteins using one-dimensional sodium dodecyl sulfate polyacrylamide gel electrophoresis (1-D SDS–PAGE) Stain-Free gels (Bio-Rad Laboratories) and polyvinylidene difluoride (PVDF) membranes (GE Healthcare, Mississauga, Canada) as an alternative to the most common normalization method using housekeeping proteins. Stain-Free technology enables fluorescent visualization of 1-D SDS–PAGE gels and corresponding blots under UV light using the Gel Doc Imaging System (Bio-Rad Laboratories). This technology has a linear dynamic detection range [35,36]. The relative amount of total proteins in each lane on the blots was calculated with the Quantity One software version 4.3.0 (Bio-Rad Laboratories) using the Volumes tool. The PVDF membranes were then blocked with 5% non-fat dry milk/Tween-0.1% in PBS and successively incubated with a primary antibody against caveolin-1 (CAV1; rabbit polyclonal, 1:1,000; Cell Signaling, Whitby, Canada) or MCT4 (rabbit polyclonal, 1:1,000; Santa Cruz Biotechnology, Dallas, TX), and a secondary antibody anti-rabbit coupled to horseradish peroxidase for visualization (1:10,000; Jackson ImmunoResearch Laboratories, West Grove, PA). Immunoreactive complexes were revealed with an enhanced chemiluminescence (ECL) western blotting substrate (GE Healthcare) and the Fluor S-Max Imaging System (GE Healthcare). The relative amount of total CAV1 or MCT4 proteins in each lane on the blots was calculated with the Quantity One software (Bio-Rad Laboratories) using the Volumes tool. The CAV1 or MCT4 signal intensities were then normalized with the Stain-Free data.

Statistical analysis: Experimental data were presented as column bar graphs (mean ± standard error of the mean [SEM]), column mean graphs (mean ± SEM), parts of whole vertical slice graphs, or box-and-whisker plots using Prism 6 software (GraphPad Software, La Jolla, CA). In box-and-whisker plots, the central box is the interquartile range with the median indicated by the horizontal line, and the whiskers extend to the lowest and highest data values. The Student *t* test or Mann–Whitney tests were performed to determine statistical significance, and differences were considered statistically significant at a p value of less than 0.05. The sample size included data from two independent experiments performed in triplicate with biologic replicates.

RESULTS

Effect of low physiologic oxygen conditions on the gross morphology, melanogenesis, and viability of human choroidal melanocytes: To study how oxygen concentration

modulates the molecular and cellular behaviors of human choroidal melanocytes, the cells were permanently cultured under hyperoxic (21%) or physiologic (3%) oxygen conditions after the cells were isolated from the choroid layer. The cells exhibited the typical dendritic morphology of melanocytes at the two oxygen concentrations, as well as distinctive pigmentation (Figure 1A) and positivity for the melanosome marker MLANA (data not shown). The melanin content was slightly higher in the melanocytes grown at 3% O_2 (Figure 1A). Interestingly, the cellular confluency was greater at 3% O_2 in all the donors tested, even if an identical number of cells were plated at the two oxygen conditions (Figure 1A). In comparison, the UM cell morphology was similar between the two oxygen concentrations, and the confluency was slightly inferior at 3% O_2 (Figure 1B). When the viable choroidal melanocytes were counted at consecutive passages, the 3% O_2 group showed a constant increase in the number of cells compared with the hyperoxic group (Figure 2A; M1: 3.13 versus 2.28 × 10^6, p = 0.002; M2: 2.80 versus 2.13 × 10^6, p = 0.116; M3: 3.10 versus 2.40 × 10^6, p = 0.013). The UM cell counts, in contrast, were lower in the 3% O_2 group (Figure 2B; T111: 5.50 versus 2.80 × 10^6, p = 0.045; T131: 3.70 versus 2.87 × 10^6, p = 0.0004; M3: 3.10 versus 2.48 × 10^6, p = 0.028). To determine whether the oxygen concentration promotes anchorage independency in choroidal melanocytes, which is associated with cell transformation, colony formation assays were performed. No colonies were visible on any of the melanocyte plates (data not shown), compared with the UM cell plates where the colony numbers were similar between the two oxygen concentrations (Figure 2C). CAV1 upregulation plays a central role in oxidative stress-induced premature senescence [37]. This senescence marker was not significantly increased in the choroidal melanocytes grown in hyperoxia as quantified with western blotting after normalization with total proteins (Figure 3A; 4.03-, 1.37-, 1.07-fold change, respectively). The expression was also similar between the two oxygen concentrations in the UM cells (Figure 3B; 1.08-, 0.89-, and 1.16-fold change, respectively).

Low physiologic oxygen conditions shorten the doubling time of human choroidal melanocytes and increased their proliferative capacity: To comprehend how low physiologic oxygen conditions favor the expansion of choroidal melanocytes, the doubling time was calculated in the choroidal melanocytes permanently exposed to hyperoxia or 3% O_2. The doubling time was significantly faster in the cells grown at low physiologic oxygen (Figure 4A; M1: 84.9 versus 96.0

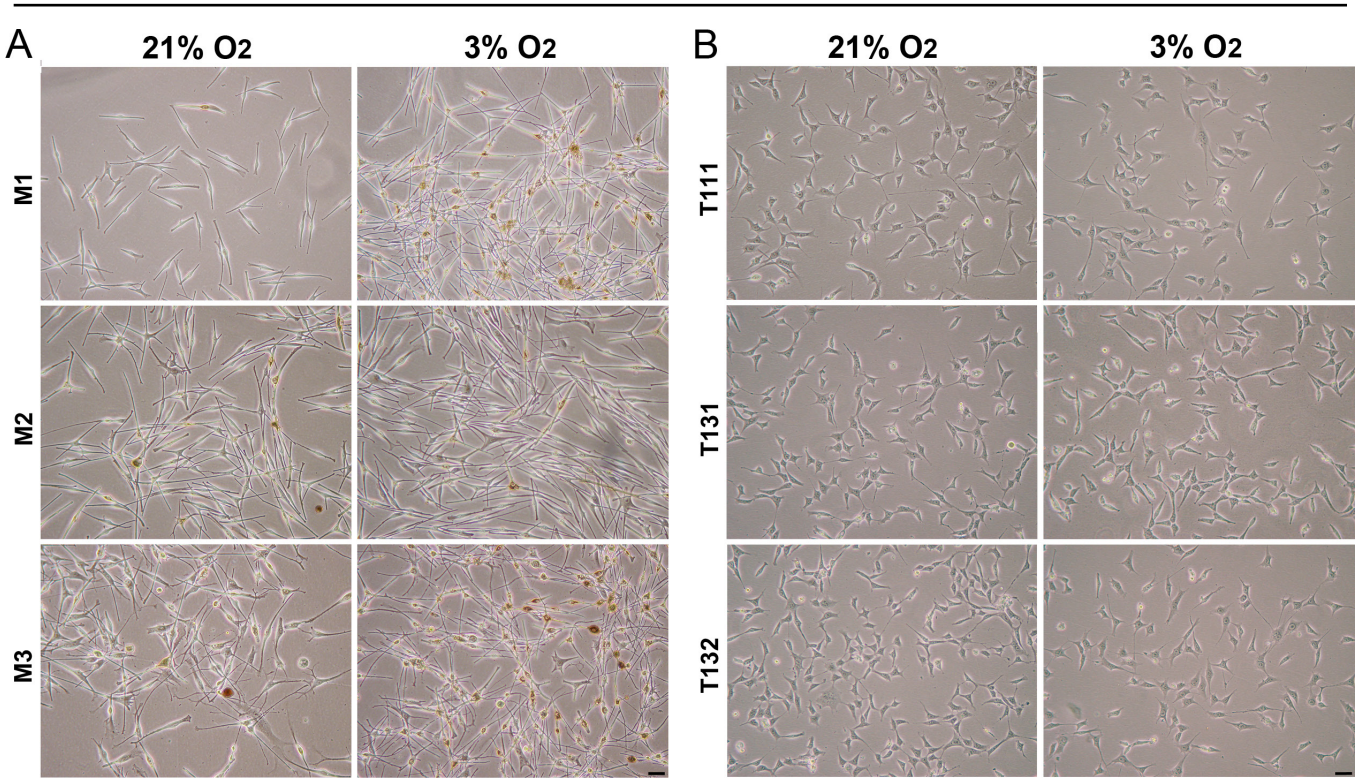

Figure 1. Low physiologic oxygen conditions favor the expansion of choroidal melanocytes. **A**: Typical morphology and melanin content of choroidal melanocytes grown under 21% or 3% O_2 (P2, 1-month exposure). **B**: Typical morphology of uveal melanoma (UM) cells grown under 21% or 3% O_2 (P2, 1-month exposure). Scale bars, 50 µm.

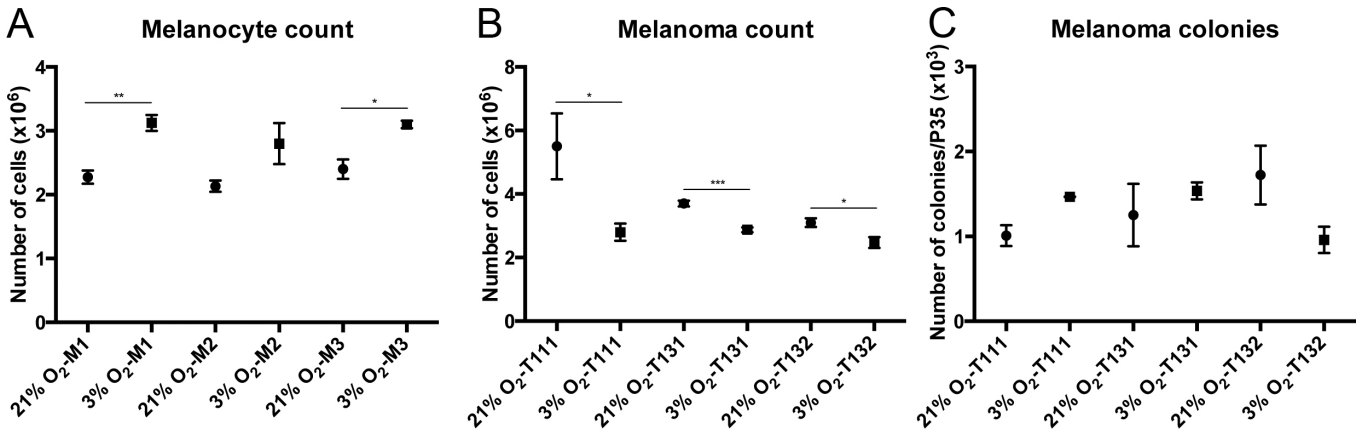

Figure 2. Low physiologic oxygen conditions improve the viability of choroidal melanocytes. **A**: Cell counts of choroidal melanocytes (n = 3) grown at 21% (•) or 3% (■) O_2 were performed at three consecutive passages using a cell and particle counter (mean ± standard error of the mean [SEM]). *p<0.05, **p<0.005, Student *t* test. **B**: Cell counts of uveal melanoma (UM) cells (n = 3) grown at 21% (•) or 3% (■) O_2 were performed at three consecutive passages using a cell and particle counter (mean ± SEM). *p<0.05, ***p<0.0005, Student *t* test. **C**: Colony counts of UM cells (n = 3) grown at 21% (•) or 3% (■) O_2 during 14 days in 1.3% methylcellulose under hyperoxia or low physiologic oxygen conditions (mean ± SEM).

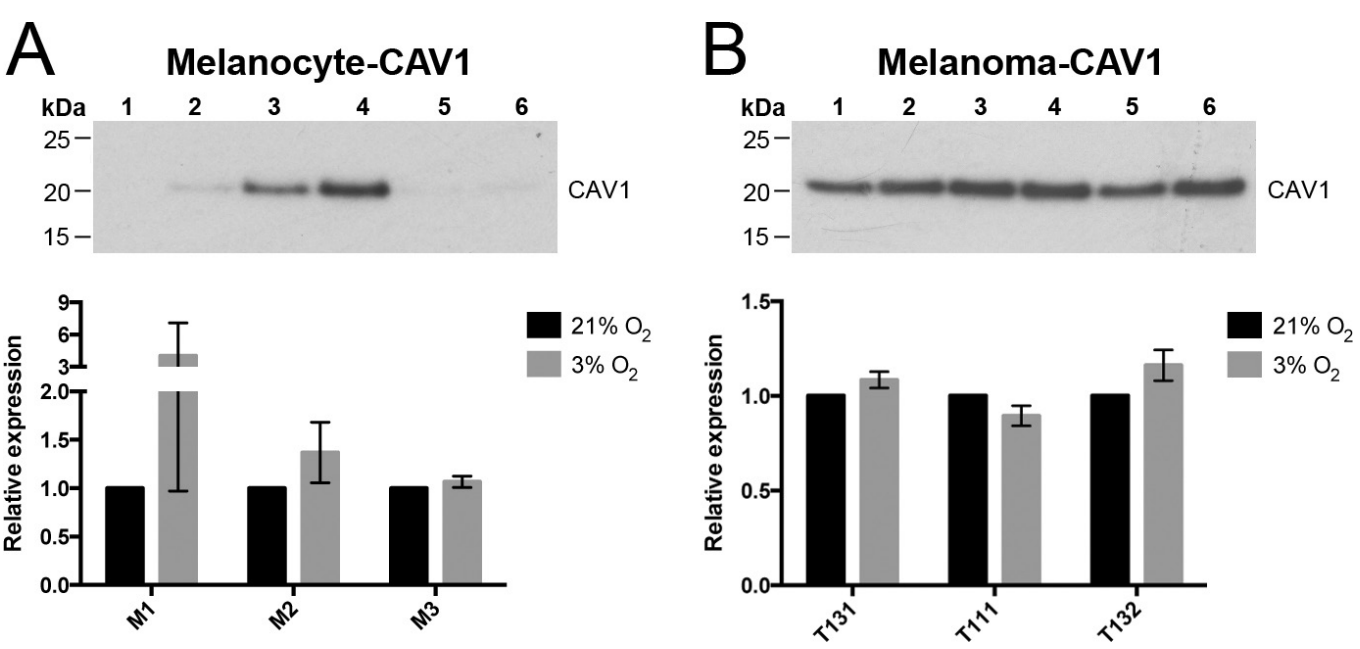

Figure 3. Low physiologic oxygen conditions do not increase cell senescence. **A**: Western blotting was conducted on protein extracts from choroidal melanocytes (n = 3) expanded at 21% (wells 1, 3, 5) or 3% (wells 2, 4, 6) O_2 using an antibody against caveolin-1 (CAV1; senescence marker, upper panel; 21 kDa). The relative amount of total CAV1 proteins per lane was calculated at 21% (black) or 3% O_2 (gray) and then normalized with the Stain-Free signal intensities. Data are presented as the expression of CAV1 using a column bar graph (lower panel; mean ± standard error of the mean [SEM]). **B**: Western blotting was conducted on protein extracts from uveal melanoma (UM) cells (n = 3) expanded at 21% (wells 1, 3, 5) or 3% (wells 2, 4, 6) O_2 using an antibody against CAV1 (upper panel). The relative amount of total CAV1 proteins per lane was calculated at 21% (black) or 3% O_2 (gray) and then normalized with the Stain-Free signal intensities. Data are presented as the expression of CAV1 using a column bar graph (lower panel; mean ± SEM).

h, p = 0.003; M2: 85.5 versus 97.6 h, p = 0.003; M3: 85.0 versus 94.0 h, p = 0.019). In comparison, the doubling time for the UM cells was slower at 3% O_2 (Figure 4C; T111: 19.6 versus 14.5 h, p = 0.019; T131: 19.1 versus 16.6 h, p = 0.0005; T132: 21.0 versus 18.3 h, p = 0.047). Next, the percentage of choroidal melanocytes in the active phases of the cell cycle was determined with immunostaining with the proliferation marker Ki67, which is absent in resting cells (the G_0 phase). The population of Ki67-positive cells was constantly greater in the choroidal melanocytes cultured at 3% O_2 (Figure 4B; M1: 40.5% versus 24.6%, p = 0.0003; M2: 36.0% versus 8.5%, p = 0.0003; M3: 38.4% versus 25.5%, p = 0.0019). The percentage of UM cells in mitosis was determined with immunostaining with the marker PH3 (the M phase), and it was similar between the two oxygen conditions (Figure 4D; T111: 2.5% versus 2.4%, p = 0.457; T131: 1.9% versus 1.4%, p = 0.0621; T132: 3.0% versus 3.4%, p = 0.262). Gross observation of the melanocyte nuclei in immunofluorescence pointed to some differences in the size and shape of the nucleus between the two oxygen concentrations. The circularity and area (μm^2) of the choroidal melanocyte nuclei were thus measured using ImageJ. As shown in Figure 5A, the nuclei of the cells exposed to low physiologic oxygen were rounder (circularity values closer to 1) than those of the melanocytes grown in hyperoxia, coherent with an increase in DNA synthesis. In addition, the nuclei of the 3% O_2 group were also bigger than those of the 21% O_2 group (Figure 5B), consistent with the fact that the nucleus increases in volume throughout the cell cycle in concert with cell growth.

Low physiologic oxygen conditions increase the mRNA and protein expression of lactate transporter MCT4 in human choroidal melanocytes: We thus hypothesized that oxygen modulates the cell behaviors of choroidal melanocytes by changing their transcriptome. To evaluate such a possibility, variations at the transcriptional level between choroidal melanocytes permanently grown at 21% or 3% O_2 were assessed using gene expression profiling. Surprisingly, scatterplot analysis of the targets that cover the entire human transcriptome indicated that the 21% and 3% O_2 groups shared larger similarities than predicted, as indicated by the variation in the slope of the regression curve (R^2 = 0.8827–0.9790; Figure 6A). The number of deregulated transcripts between the two oxygen conditions is compiled in Table 1 for each donor (fold change >2 or <0.5). Interestingly, the expression of HIF1A and HIF2A (also called EPAS1) mRNA was not upregulated when the choroidal melanocytes were cultured at a low physiologic oxygen concentration (Figure 6B, Appendix 3). Among the transcripts containing a hypoxia-response element (HRE) listed in Figure 6B [38], VEGFA and PDK1 were upregulated at 3% O_2 in two of the three donors (fold changes >2; Appendix 3), and the CTGF, ENG, FOS, SERPINE1, and VEGFC transcripts were upregulated at 3% O_2 in one of the three donors (fold changes >2; Appendix 3). Because the cell pigmentation seemed slightly higher in the choroidal melanocytes exposed to 3% O_2 (Figure 1A), the expression of the melanocyte differentiation transcripts KIT, SOX10, PAX3, TRPM1, EDNRB, DCT, KITLG, PMEL, MITF, GPNMB, MLANA, TYR, and TYRP1 was compared between the two oxygen concentrations. As shown in Figure 6C, there was no difference in their abundance, suggesting that another molecular effect disturbs the melanin content in hyperoxia (Appendix 3). After putative genes and long non-coding RNAs targets, as well as targets with a linear signal of fluorescence intensity below 250 units were excluded, only MCT4 was found dysregulated more than a twofold change in all pairs of choroidal melanocytes. MCT4, involved in lactate transport, was upregulated in cells cultured in physiologic oxygen conditions (mean fold change of 2.4; Figure 7A). Normalization of the corresponding MCT4 linear signals with those of the housekeeping mRNA confirmed the differential gene expression between the two oxygen conditions (the mean ratio of the linear signals: 2.181 ± 0.35 versus 5.248 ± 0.69, p = 0.017; Figure 7A). Classes of transcripts statistically significantly upregulated at 3% O_2 differed between donors. For example, the interferon-related transcripts and transcripts involved in DNA or protein posttranslational modifications were overrepresented in the M1 and M3 donors, respectively. Higher expression of the MCT4 protein in the choroidal melanocytes grown at low physiologic oxygen was further confirmed with western blotting after normalization with total proteins (137.59- (p = 0.0006), 16.94- (p = 0.03), and 2.09- (p = 0.006) fold change, respectively; Figure 7B). This upregulation at 3% O_2 was also observed in two UM cell cultures (2.04- (p = 0.02) and 2.00- (p = 0.004) fold change, respectively; Figure 7B).

DISCUSSION

In tissue culture incubators, the ambient temperature and the CO_2 concentration are regulated to reflect core mammalian body temperature (37 °C) and approximate venous concentrations (5% CO_2), whereas, in striking contrast, the oxygen concentration is not adjusted to physiologic levels (2–9% O_2). Previous observations in cultured cells [9,11-18,39] should prompt us to routinely implement low physiologic oxygen conditions as an essential parameter in experiments performed in vitro. However, even today, only a few studies have been conducted by growing differentiated cells permanently at reduced oxygen to reproduce their in situ environment and draw valid conclusions about their

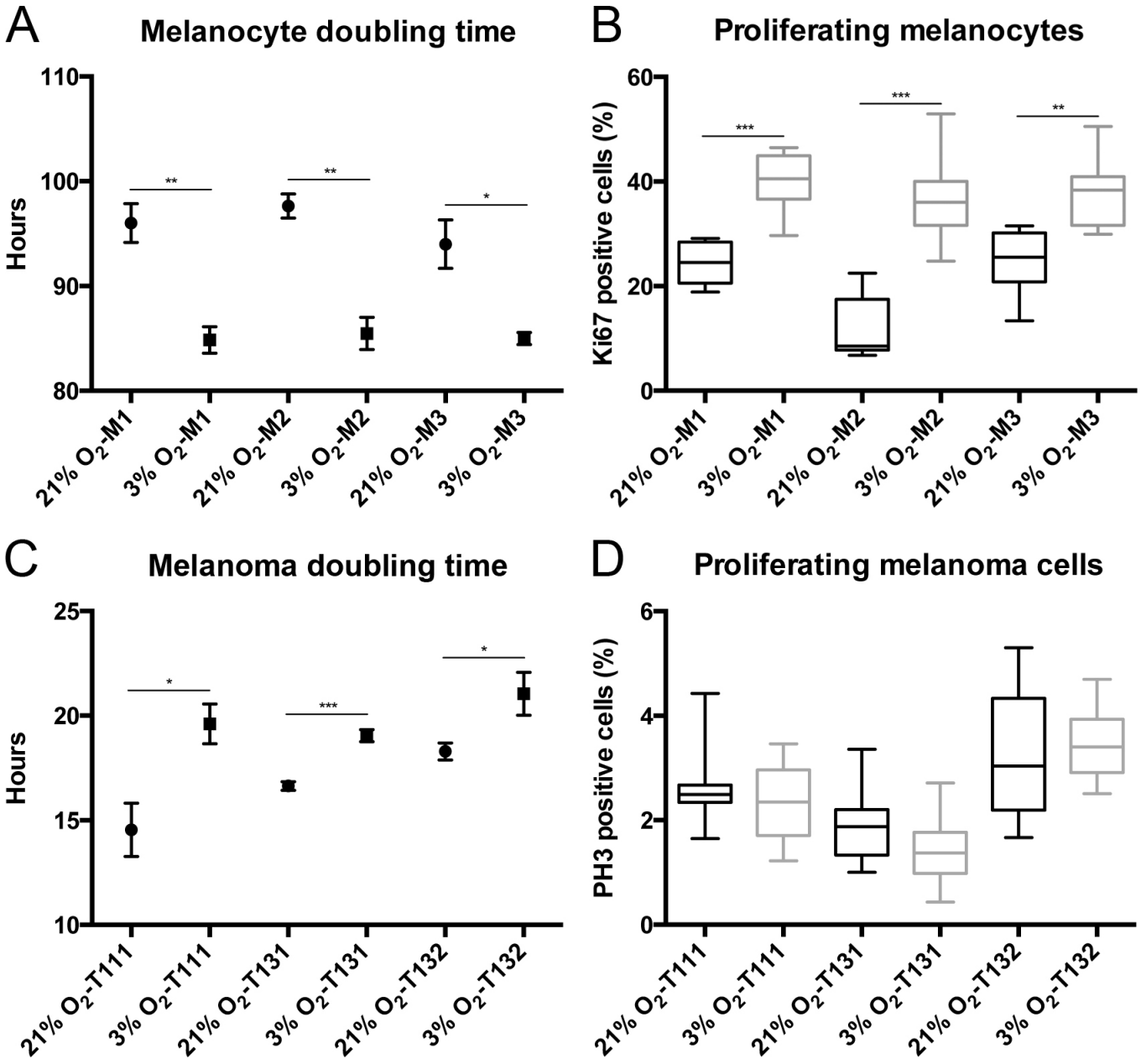

Figure 4. Low physiologic oxygen conditions shorten the doubling time of choroidal melanocytes and increase their proliferative capacity. **A**: The doubling time of the choroidal melanocytes (n = 3) expanded under 21% (•) or 3% (■) O_2 conditions was determined at three consecutive passages (mean ± standard error of the mean [SEM]). *p<0.05, **p<0.005, the Student *t* test. **B**: The percentage of choroidal melanocytes (n = 3) in the active phases of the cell cycle was determined with immunofluorescence analyses using Ki67 on cells exposed to 21% (black) or 3% (gray) O_2. The Ki67-positive cells were counted, and the total number of 4',6-diamidino-2-phenylindole (DAPI)-stained nuclei was used for normalization. **p<0.005, ***p<0.0005, Mann–Whitney test. **C**: The doubling time of uveal melanoma (UM) cells (n = 3) cultured under 21% (•) or 3% (■) O_2 conditions was determined at three consecutive passages (mean ± SEM). *p<0.05, ***p<0.0005, the Student *t* test. **D**: The percentage of UM cells (n = 3) in the mitotic phase of the cell cycle was determined with immunofluorescence analyses using phosphohistone H3 (PH3) on cells exposed to 21% (black) or 3% (gray) O_2. The PH3-positive cells were counted, and the total number of DAPI-stained nuclei was used for normalization.

physiology. Thus, exposing cells at low physiologic oxygen concentrations dramatically affects their phenotype through modification of cellular functions, such as the proliferation rate in lymphocytes [9,15], myoblasts [14], skeletal muscle satellite cells [11,18], and neuron precursors [17], as well as the phagocytic capacity of macrophages [13]. Low physiologic oxygen concentrations also statistically significantly impact metabolism, redox status, and gene expression [12,16,39]. As far as we are aware, only one study previously reported transcriptome data from one uveal melanocyte cell line cultured under atmospheric oxygen concentrations [40]. No studies have been performed to examine at the molecular level the effects of reduced oxygen on ocular melanocytes. Although at first we could not predict how well our cells would survive in long-term culture under low physiologic oxygen conditions, we were somewhat surprised to find that the choroidal melanocytes happily grew at 3% O_2. We showed that a physiologic oxygen concentration allowed optimization of the choroidal melanocyte expansion by shortening their doubling time, by increasing the population of cells in the active phases of the cell cycle (Ki67 positive), and by upregulating the expression of the lactate transporter MCT4. In addition, we are the first to report gene expression profiling data for choroidal melanocytes grown at low physiologic oxygen conditions.

The melanocyte-specific transcription factor MITF was shown to bind directly to the HIF1A promoter and control its gene expression through cAMP stimulation in skin melanocytes, independently of the oxygen conditions, suggesting that HIF1A plays a prosurvival role in this cell type [41]. The cAMP pathway induces pigmentation by controlling several

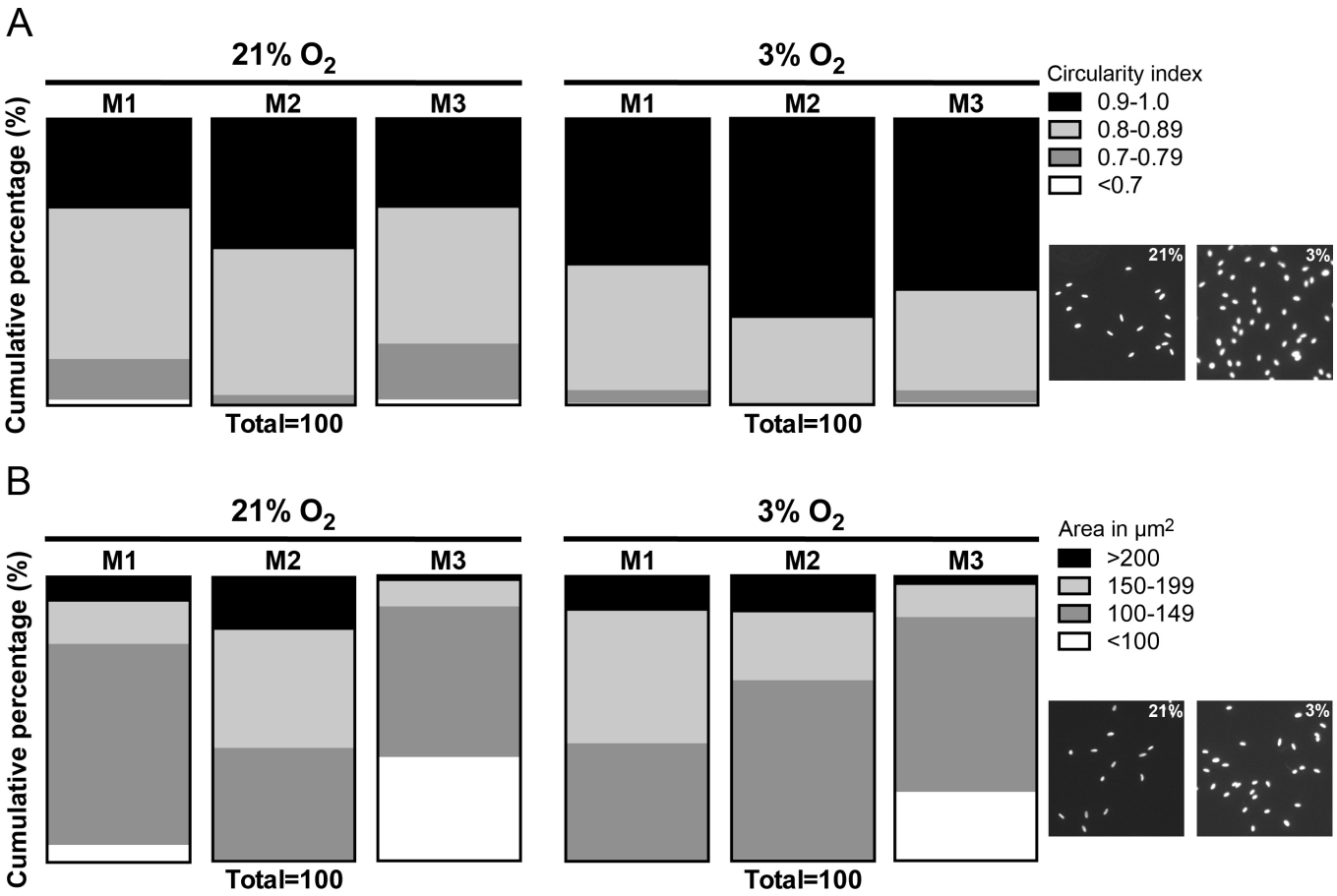

Figure 5. Low physiologic oxygen conditions are associated with the greater size and circularity of choroidal melanocyte nuclei. **A**: Circularity of the nuclei was determined in choroidal melanocytes exposed at 21% or 3% O_2 (n = 3) by analyzing a minimum of 500 nuclei per condition with ImageJ and the following formula: $4\pi \times [\text{Area}] / [\text{Perimeter}]^2$. The circularity ranged from 0 (infinitely elongated polygon) to 1 (perfect circle). **B**: The area of the nucleus (µm^2) was measured in choroidal melanocytes grown under hyperoxia and low physiologic oxygen conditions by analyzing a minimum of 500 nuclei per condition with ImageJ. Data are presented as a cumulative percentage using parts of whole vertical slice graphs. Representative fields of DAPI-stained nuclei of choroidal melanocytes exposed to 21% or 3% O_2 are shown on the right-hand side of the panels.

Table 1. Number of deregulated transcripts between both oxygen conditions for each donor.

Donor	Upregulated Transcripts (3% O_2) (fold-change >2)	Downregulated Transcripts (3% O_2) (fold-change <0.5)
M1	1,869	1,954
M2	838	896
M3	3,275	2,996

parameters of melanocyte differentiation, such as melanin synthesis and dendrite outgrowth [42,43]. In the present study, expression of HIF1A and HIF2A mRNAs was not upregulated when the choroidal melanocytes were cultured at 3% O_2, implying that these experiments were conducted when cells had already adapted to the reduced oxygen conditions. However, the expression of many HIF targets was significantly increased in all donors. The choroidal melanocytes were slightly more pigmented in the physiologic oxygen conditions. The gene expression profiling did not show an increase in the expression of the melanocyte differentiation master regulator MITF or the enzymes TYR, DCT, and TYRP1 involved in melanogenesis. These results indicate that hyperoxia may affect melanocyte differentiation by other molecular mechanisms, for example, melanin maturation. It was previously shown that low physiologic oxygen concentrations promote cutaneous melanocyte proliferation and tyrosinase activity [44].

It is known that mild and prolonged hyperoxia causes ROS production and oxidative damage to lipids, carbohydrates, proteins, and DNA, which have drastic consequences on cell physiology [45]. Hyperoxia can also increase the rate of telomere shortening and lead to cell cycle exit in senescence [46]. Permanent culturing of choroidal melanocytes at 21% O_2 significantly affected their viability, likely by inducing hyperoxic oxidative stress. However, we did not find more senescent melanocytes with gross microscopic observation or with western blotting with the senescence marker CAV1. HIF1A plays a role in anchorage-independent

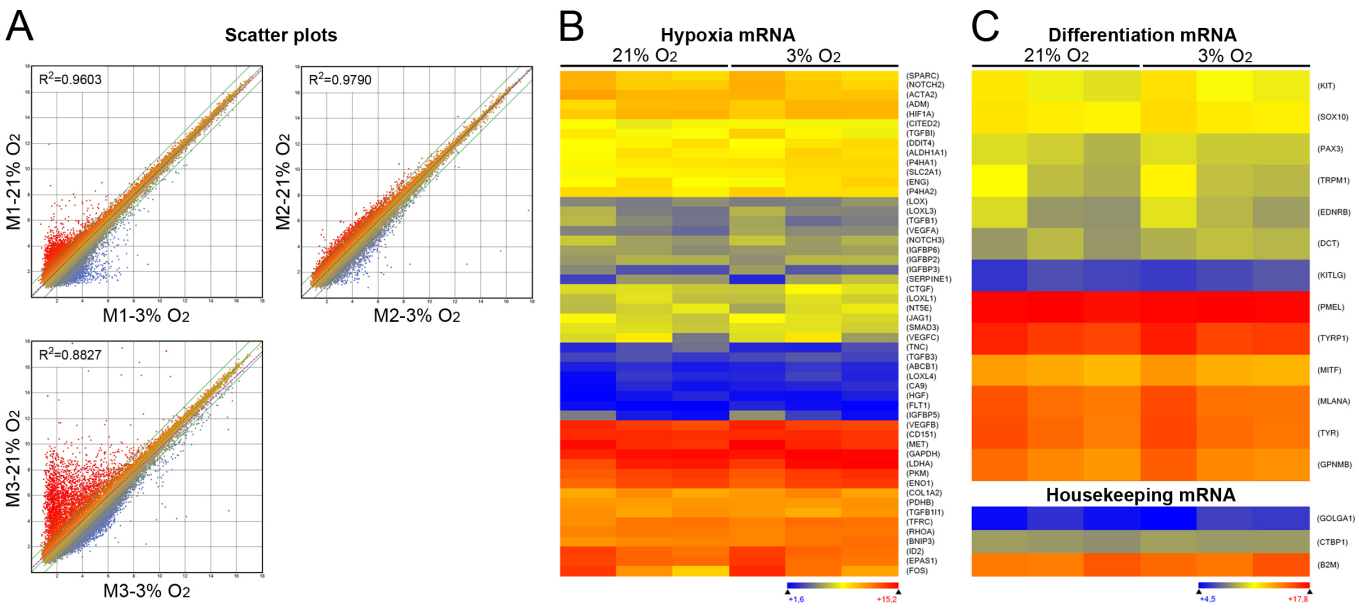

Figure 6. Low physiologic oxygen conditions change slightly the transcriptome of choroidal melanocytes. **A**: Scatterplots of signal intensity in $\log_2$ from 60,000 different targets covering the entire human transcriptome of choroidal melanocytes (n = 3) exposed to hyperoxia (the y-axis) plotted against their counterpart grown under low physiologic oxygen conditions (the x-axis). The twofold change in intensity lines is shown in green. The displacement of the linear regression curve (dashed purple) away from the central axis reflects the degree of divergence in the pattern of gene expression between the two oxygen conditions (R^2 value, coefficient of determination). **B**: Heatmap representation of mRNAs containing a hypoxia-response element expressed by choroidal melanocytes expanded at 21% or 3% O_2. **C**: Heatmap representation of mRNAs linked to melanocyte differentiation expressed by choroidal melanocytes expanded at 21% or 3% O_2. Data are also presented for the housekeeping mRNA golgin A1 (GOLGA1), C-terminal binding protein 1 (CTBP1), and beta-2-microglobulin (B2M). Transcripts indicated in dark blue correspond to those whose expression is low, whereas highly expressed transcripts are shown in orange and red.

survival, a feature that is modeled in vitro by colony formation in agar or methylcellulose suspension [47]. Using this method, we ruled out the transformation of choroidal melanocytes exposed at 3% O_2. Together, these results suggest that the decline in viability and the cell counts encountered in hyperoxia may lie in molecular mechanisms that control the cell cycle or DNA repair. Interestingly, we did not measure a significant increase in the colony number for the UM cells exposed to 3% O_2. Moreover, hypoxic conditions (<1% O_2) might favor the self-renewal of UM cells in accordance with the theory of cancer stem cells [48].

One feature commonly noted in many cell types cultured under low physiologic oxygen concentration is a higher proliferation rate [9,11,14,15,17,18], but the underlying mechanisms by which it is promoted are currently unknown. We found more choroidal melanocytes positive for the proliferation marker Ki67 at 3% O_2, and their doubling time was also shorter. Nuclear shape and size are among the characteristics that could be used to study cell differentiation, development, or disease [49,50]. In addition, the nucleus of the proliferating cells increases between one mitosis phase and the next [50]. Interestingly, the low physiologic oxygen concentration was correlated with the greater size and circularity of the cell nuclei in our study. Cells exposed to hyperoxia become more elongated [51], and this alteration of the nuclear shape induces conformational changes in chromatin, thus affecting DNA synthesis, and cell proliferation [52]. In addition, there is an important cell cycle checkpoint that takes place within the

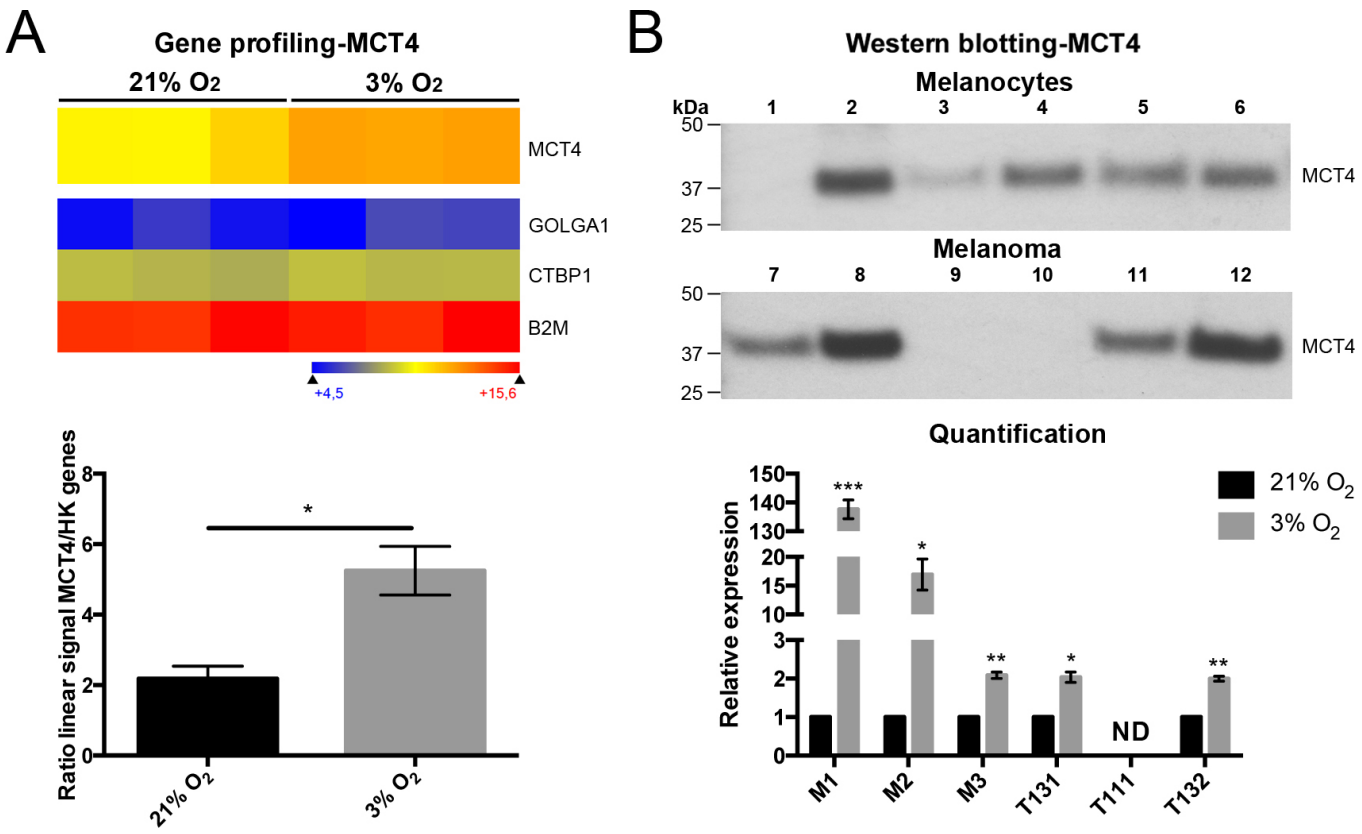

Figure 7. Low physiologic oxygen conditions increased the mRNA and protein expression of lactate transporter MCT4 in choroidal melanocytes. **A**: Heatmap representation of monocarboxylate transporter (MCT4) expressed by choroidal melanocytes grown at 21% or 3% O_2 (n = 3/group). Data are also presented for the housekeeping mRNA golgin A1 (GOLGA1), C-terminal binding protein 1 (CTBP1), and beta-2-microglobulin (B2M) (upper panel). Transcripts indicated in dark blue correspond to those whose expression is low, whereas the highly expressed transcripts are shown in orange and red. Corresponding linear signals obtained for the MCT4 mRNA at 21% (black) or 3% (gray) O_2 and normalized with the housekeeping mRNA are displayed as the ratio of the linear signals using a column bar graph (lower panel; mean ± standard error of the mean [SEM]). *p<0.05, Student *t* test. **B**: Western blotting conducted on protein extracts from choroidal melanocytes (M1–M3) or uveal melanoma (UM) cells (T111, T131, T132) expanded at 21% (odd numbers) or 3% (even numbers) O_2 (n = 3/group) using an antibody against MCT4 (upper panel; 43 kDa). The relative amount of total MCT4 protein per lane was calculated at 21% (black) or 3% (gray) O_2 and then normalized with the Stain-Free signal intensities. Data are presented as relative expression of MCT4 using a column bar graph (lower panel; mean ± SEM). *p<0.05, ** p<0.01, ***p<0.001, Student *t* test. ND, no detectable bands.

G2/M transition, to scrutinize the cell's DNA and make sure it is structurally intact and properly replicated. We suggest that the choroidal melanocytes grown at 21% O_2 may pause longer at this point to allow time for DNA repair after they are exposed to hyperoxic oxidative stress. Therefore, to better understand the differential cell cycle regulation by reduced oxygen and hyperoxia, an extensive study of the activity of the cell cycle progression factors is required (i.e., specific cyclins/cyclin-dependent kinases and phosphorylation of their targets).

MCT4 is a plasma membrane transporter that catalyzes a proton-coupled transport of lactate and other monocarboxylates for the facilitation of continued glycolytic ATP production [53,54]. The expression of MCT4 is restricted to astrocytes, lymphocytes, and muscle fiber cells among healthy cells [53] and is induced in low oxygen through HIF1A to contribute to intracellular pH regulation [55]. MCT4 was the only mRNA statistically significantly upregulated at 3% O_2 in all donors according to the DNA microarray analysis. To the best of our knowledge, we are the first to identify MCT4 in ocular melanocytes. Its chaperone basigin, required for correct plasma membrane expression, was among the transcripts with intermediate-level expression in the choroidal melanocytes but was not increased at 3% O_2. We suggest that the proliferating choroidal melanocytes have increased glucose uptake and lactate production; therefore, MCT4 expression and activity were regulated accordingly in these cells. In addition, the lactate ion is considered a potential antioxidant agent that can, for example, inhibit lipid peroxidation [56]. We propose that choroidal melanocytes at low physiologic oxygen conditions release more lactate in the extracellular space and therefore have a more effective antioxidant defense.

Studies that used atmospheric oxygen concentrations for tissue culture have yielded much valuable information; the present study suggests, however, that efforts to reproduce the physiologic cell environment of choroidal melanocytes will lead to a significantly improved research outcome with less artifactual results, especially when this cell type is used as an in vitro model for choroidal pathologies, such as uveal melanoma. Additional studies using a range of oxygen concentrations are needed to refine the optimal percentage for choroidal melanocytes. Further investigation of the molecular mechanisms regulating cell physiology in hyperoxia and reduced oxygen concentrations will allow better understanding of the adaptation of cells to oxygen variations. For instance, the accumulation of irreversible oxidative damages to biomolecules, dysregulation of posttranslational modifications on proteins involved in cell cycle progression, as well as reduced MCT4 activity, could play a role in the decreased viability and proliferation observed in choroidal melanocytes cultured under hyperoxia.

APPENDIX 1. CLINICOPATHOLOGICAL FEATURES AND SURVIVAL DATA OF UVEAL MELANOMA CASES.

To access the data, click or select the words "Appendix 1."

APPENDIX 2. CHARACTERISTICS OF CELL CULTURES DERIVED FROM UM PRIMARY TUMORS.

To access the data, click or select the words "Appendix 2." Phase contrast micrographs of monolayer cultures of UM cells T111, T131 and T132 and their expression of MLANA. Dark brown indicates positive staining. The primary antibody was omitted as negative control. Scale bars, 20 µm.

APPENDIX 3. LINEAR SIGNALS OF GENES APPEARING ON HEATMAPS.

To access the data, click or select the words "Appendix 3."

ACKNOWLEDGMENTS

The authors would like to thank Renée Paradis, Florence Pagé-Larivière, and Julie Bérubé for technical assistance, as well as Dr. Karine Zaniolo from the Plateforme de génétique moléculaire du CUO-Recherche. S.L. is a Research Scholar of Fonds de recherche du Québec - Santé (FRQS). C.W. is a recipient of a Doctoral Training Award from the Fondation du CHU de Québec. J.P. and L.T.V. are recipients of Master Training Awards from FRQS. C.W. and L.T.V. are recipients of Training Awards from the Centre de recherche en organogénèse expérimentale de l'Université Laval/LOEX, and the Faculté de médecine de l'Université Laval. J.P. is a recipient of a Training Award from Diabète Québec. This work was supported by grants from the FRQS, Canadian Foundation for Innovation, Fondation du CHU de Québec, Fondation "Ophtalmologie, Recherche et Développement", Fondation des maladies de l'oeil and Fondation de l'Université Laval. The Eye Tissue Bank and Uveal Melanoma Biobank are financially supported by the FRQS Vision Health Research Network.

REFERENCES

1. Yla-Herttuala S. Oxidized LDL and atherogenesis. Ann N Y Acad Sci 1999; 874:134-7. [PMID: 10415527].
2. Stadtman ER, Levine RL. Protein oxidation. Ann N Y Acad Sci 2000; 899:191-208. [PMID: 10863540].

3. Marnett LJ. Oxyradicals and DNA damage. Carcinogenesis 2000; 21:361-70. [PMID: 10688856].
4. Finkel T, Holbrook NJ. Oxidants, oxidative stress and the biology of ageing. Nature 2000; 408:239-47. [PMID: 11089981].
5. Semenza GL. Regulation of oxygen homeostasis by hypoxia-inducible factor 1. Physiology (Bethesda) 2009; 24:97-106. [PMID: 19364912].
6. Kuschel A, Simon P, Tug S. Functional regulation of HIF-1alpha under normoxia–is there more than post-translational regulation? J Cell Physiol 2012; 227:514-24. [PMID: 21503885].
7. Simon MC, Keith B. The role of oxygen availability in embryonic development and stem cell function. Nat Rev Mol Cell Biol 2008; 9:285-96. [PMID: 18285802].
8. Carreau A, El Hafny-Rahbi B, Matejuk A, Grillon C, Kieda C. Why is the partial oxygen pressure of human tissues a crucial parameter? Small molecules and hypoxia. J Cell Mol Med 2011; 15:1239-53. [PMID: 21251211].
9. Carswell KS, Weiss JW, Papoutsakis ET. Low oxygen tension enhances the stimulation and proliferation of human T lymphocytes in the presence of IL-2. Cytotherapy 2000; 2:25-37. [PMID: 12042052].
10. Ivanovic Z. Hypoxia or in situ normoxia: The stem cell paradigm. J Cell Physiol 2009; 219:271-5. [PMID: 19160417].
11. Csete M, Walikonis J, Slawny N, Wei Y, Korsnes S, Doyle JC, Wold B. Oxygen-mediated regulation of skeletal muscle satellite cell proliferation and adipogenesis in culture. J Cell Physiol 2001; 189:189-96. [PMID: 11598904].
12. Parrinello S, Samper E, Krtolica A, Goldstein J, Melov S, Campisi J. Oxygen sensitivity severely limits the replicative lifespan of murine fibroblasts. Nat Cell Biol 2003; 5:741-7. [PMID: 12855956].
13. Grodzki AC, Giulivi C, Lein PJ. Oxygen tension modulates differentiation and primary macrophage functions in the human monocytic THP-1 cell line. PLoS One 2013; 8:e54926-[PMID: 23355903].
14. Duguez S, Duddy WJ, Gnocchi V, Bowe J, Dadgar S, Partridge TA. Atmospheric oxygen tension slows myoblast proliferation via mitochondrial activation. PLoS One 2012; 7:e43853-[PMID: 22937109].
15. Atkuri KR, Herzenberg LA, Niemi AK, Cowan T, Herzenberg LA. Importance of culturing primary lymphocytes at physiological oxygen levels. Proc Natl Acad Sci USA 2007; 104:4547-52. [PMID: 17360561].
16. Alvarez K, de Andres MC, Takahashi A, Oreffo RO. Effects of hypoxia on anabolic and catabolic gene expression and DNA methylation in OA chondrocytes. BMC Musculoskelet Disord 2014; 15:431-[PMID: 25510649].
17. Studer L, Csete M, Lee SH, Kabbani N, Walikonis J, Wold B, McKay R. Enhanced proliferation, survival, and dopaminergic differentiation of CNS precursors in lowered oxygen. J Neurosci 2000; 20:7377-83. [PMID: 11007896].
18. Chakravarthy MV, Spangenburg EE, Booth FW. Culture in low levels of oxygen enhances in vitro proliferation potential of satellite cells from old skeletal muscles. Cell Mol Life Sci 2001; 58:1150-8. [PMID: 11529507].
19. Boissy RE. The melanocyte. Its structure, function, and subpopulations in skin, eyes, and hair. Dermatol Clin 1988; 6:161-73. [PMID: 3288380].
20. Thomas AJ, Erickson CA. The making of a melanocyte: the specification of melanoblasts from the neural crest. Pigment Cell Melanoma Res 2008; 21:598-610. [PMID: 19067969].
21. Sarna T. Properties and function of the ocular melanin–a photobiophysical view. J Photochem Photobiol B 1992; 12:215-58. [PMID: 1635010].
22. Hu DN. Photobiology of ocular melanocytes and melanoma. Photochem Photobiol 2005; 81:506-9. [PMID: 15496134].
23. Schraermeyer U, Heimann K. Current understanding on the role of retinal pigment epithelium and its pigmentation. Pigment Cell Res 1999; 12:219-36. [PMID: 10454290].
24. Hu DN, McCormick SA, Ritch R. Studies of human uveal melanocytes in vitro: growth regulation of cultured human uveal melanocytes. Invest Ophthalmol Vis Sci 1993; 34:2220-7. [PMID: 7685008].
25. Hu DN, McCormick SA, Ritch R, Pelton-Henrion K. Studies of human uveal melanocytes in vitro: isolation, purification and cultivation of human uveal melanocytes. Invest Ophthalmol Vis Sci 1993; 34:2210-9. [PMID: 8505203].
26. Ahmed J, Braun RD, Dunn R Jr, Linsenmeier RA. Oxygen distribution in the macaque retina. Invest Ophthalmol Vis Sci 1993; 34:516-21. [PMID: 8449672].
27. Birol G, Wang S, Budzynski E, Wangsa-Wirawan ND, Linsenmeier RA. Oxygen distribution and consumption in the macaque retina. Am J Physiol Heart Circ Physiol 2007; 293:H1696-704. [PMID: 17557923].
28. Yu DY, Cringle SJ, Su EN. Intraretinal oxygen distribution in the monkey retina and the response to systemic hyperoxia. Invest Ophthalmol Vis Sci 2005; 46:4728-33. [PMID: 16303972].
29. Bergeron MA, Champagne S, Gaudreault M, Deschambeault A, Landreville S. Repression of genes involved in melanocyte differentiation in uveal melanoma. Mol Vis 2012; 18:1813-22. [PMID: 22815634].
30. Mouriaux F, Sanschagrin F, Diorio C, Landreville S, Comoz F, Petit E, Bernaudin M, Rousseau AP, Bergeron D, Morcos M. Increased HIF-1alpha expression correlates with cell proliferation and vascular markers CD31 and VEGF-A in uveal melanoma. Invest Ophthalmol Vis Sci 2014; 55:1277-83. [PMID: 24481264].
31. Landreville S, Agapova OA, Kneass ZT, Salesse C, Harbour JW. ABCB1 identifies a subpopulation of uveal melanoma cells with high metastatic propensity. Pigment Cell Melanoma Res 2011; 24:430-7. [PMID: 21575142].
32. Heppner FL, Roth K, Nitsch R, Hailer NP. Vitamin E induces ramification and downregulation of adhesion molecules

in cultured microglial cells. Glia 1998; 22:180-8. [PMID: 9537838].

33. Landreville S, Vigneault F, Bergeron MA, Leclerc S, Gaudreault M, Morcos M, Mouriaux F, Salesse C, Guerin SL. Suppression of alpha5 gene expression is closely related to the tumorigenic properties of uveal melanoma cell lines. Pigment Cell Melanoma Res 2011; 24:643-55. [PMID: 21592318].

34. Lee S, Jo M, Lee J, Koh SS, Kim S. Identification of novel universal housekeeping genes by statistical analysis of microarray data. J Biochem Mol Biol 2007; 40:226-31. [PMID: 17394773].

35. Gilda JE, Gomes AV. Western blotting using in-gel protein labeling as a normalization control: stain-free technology. Methods Mol Biol 2015; 1295:381-91. [PMID: 25820735].

36. Posch A, Kohn J, Oh K, Hammond M, Liu N. V3 stain-free workflow for a practical, convenient, and reliable total protein loading control in western blotting. J Vis Exp 2013; •••:50948-[PMID: 24429481].

37. Zou H, Stoppani E, Volonte D, Galbiati F. Caveolin-1, cellular senescence and age-related diseases. Mech Ageing Dev 2011; 132:533-42. [PMID: 22100852].

38. Wenger RH, Stiehl DP, Camenisch G. Integration of oxygen signaling at the consensus HRE. Sci STKE 2005; 2005:re12-.

39. Halliwell B. Oxidative stress in cell culture: an under-appreciated problem? FEBS Lett 2003; 540:3-6. [PMID: 12681474].

40. An J, Wan H, Zhou X, Hu DN, Wang L, Hao L, Yan D, Shi F, Zhou Z, Wang J, Hu S, Yu J, Qu J. A comparative transcriptomic analysis of uveal melanoma and normal uveal melanocyte. PLoS One 2011; 6:e16516-[PMID: 21305041].

41. Busca R, Berra E, Gaggioli C, Khaled M, Bille K, Marchetti B, Thyss R, Fitsialos G, Larribere L, Bertolotto C, Virolle T, Barbry P, Pouyssegur J, Ponzio G, Ballotti R. Hypoxia-inducible factor 1{alpha} is a new target of microphthalmia-associated transcription factor (MITF) in melanoma cells. J Cell Biol 2005; 170:49-59. [PMID: 15983061].

42. Busca R, Ballotti R. Cyclic AMP a key messenger in the regulation of skin pigmentation. Pigment Cell Res 2000; 13:60-9. [PMID: 10841026].

43. Busca R, Bertolotto C, Abbe P, Englaro W, Ishizaki T, Narumiya S, Boquet P, Ortonne JP, Ballotti R. Inhibition of Rho is required for cAMP-induced melanoma cell differentiation. Mol Biol Cell 1998; 9:1367-78. [PMID: 9614180].

44. Horikoshi T, Balin AK, Carter DM. Effects of oxygen tension on the growth and pigmentation of normal human melanocytes. J Invest Dermatol 1991; 96:841-4. [PMID: 1904467].

45. Kulkarni AC, Kuppusamy P, Parinandi N. Oxygen, the lead actor in the pathophysiologic drama: enactment of the trinity of normoxia, hypoxia, and hyperoxia in disease and therapy. Antioxid Redox Signal 2007; 9:1717-30. [PMID: 17822371].

46. von Zglinicki T, Saretzki G, Docke W, Lotze C. Mild hyperoxia shortens telomeres and inhibits proliferation of fibroblasts: a model for senescence? Exp Cell Res 1995; 220:186-93. [PMID: 7664835].

47. Rohwer N, Welzel M, Daskalow K, Pfander D, Wiedenmann B, Detjen K, Cramer T. Hypoxia-inducible factor 1alpha mediates anoikis resistance via suppression of alpha5 integrin. Cancer Res 2008; 68:10113-20. [PMID: 19074877].

48. Keith B, Simon MC. Hypoxia-inducible factors, stem cells, and cancer. Cell 2007; 129:465-72. [PMID: 17482542].

49. Jevtic P, Edens LJ, Vukovic LD, Levy DL. Sizing and shaping the nucleus: mechanisms and significance. Curr Opin Cell Biol 2014; 28:16-27. [PMID: 24503411].

50. Walters AD, Bommakanti A, Cohen-Fix O. Shaping the nucleus: factors and forces. J Cell Biochem 2012; 113:2813-21. [PMID: 22566057].

51. McGrath-Morrow SA, Stahl J. Growth arrest in A549 cells during hyperoxic stress is associated with decreased cyclin B1 and increased p21(Waf1/Cip1/Sdi1) levels. Biochim Biophys Acta 2001; 1538:90-7. [PMID: 11341986].

52. Versaevel M, Grevesse T, Gabriele S. Spatial coordination between cell and nuclear shape within micropatterned endothelial cells. Nat Commun 2012; 3:671-[PMID: 22334074].

53. Halestrap AP. The SLC16 gene family - structure, role and regulation in health and disease. Mol Aspects Med 2013; 34:337-49. [PMID: 23506875].

54. Halestrap AP, Price NT. The proton-linked monocarboxylate transporter (MCT) family: structure, function and regulation. Biochem J 1999; 343:281-99. [PMID: 10510291].

55. Ullah MS, Davies AJ, Halestrap AP. The plasma membrane lactate transporter MCT4, but not MCT1, is up-regulated by hypoxia through a HIF-1alpha-dependent mechanism. J Biol Chem 2006; 281:9030-7. [PMID: 16452478].

56. Groussard C, Morel I, Chevanne M, Monnier M, Cillard J, Delamarche A. Free radical scavenging and antioxidant effects of lactate ion: an in vitro study. J Appl Physiol 2000; 89:169-75. [PMID: 10904049].

Articles are provided courtesy of Emory University and the Zhongshan Ophthalmic Center, Sun Yat-sen University, P.R. China. The print version of this article was created on 12 March 2017. This reflects all typographical corrections and errata to the article through that date. Details of any changes may be found in the online version of the article.